27th EPS Conference on Contr. Fusion and Plasma Phys. Budapest, 12-16 June 2000 ECA Vol. **24B** (2000) 312 -315

# Sawtooth magnetic reconnection with localised plasma heating

**F. Porcelli**[1,2], C. Angioni[1], R. Behn[1], I. Furno[1], T. Goodman[1], M. Henderson[1], Z. A. Pietrzyk[1], A. Pochelon[1], H. Reimerdes[1], E. Rossi[3] and O. Sauter[1]

[1] CRPP, Ass. Euratom - Conf. Suisse, EPFL, Switzerland

[2] Istituto Nazionale Fisica della Materia, Politecnico di Torino, Italy

[3] Institute for Fusion Studies, University of Texas at Austin, USA

**Abstract**

An interpretation of nonstandard, central magneto-hydro-dynamic (MHD) events in the Tokamak à Configuration Variable (TCV) during localized Electron Cyclotron Resonant Heating (ECRH) is presented.

Tokamak experiments with localised ECRH have revealed peculiar plasma behavior. One example is the observation of multipeaked electron temperature profiles and sharp temperature gradients in RTP [1] and TEXT-U [2] experiments, explained in Ref. [3] as the consequence of the interaction between ECRH and resistive MHD m=1 modes, which are responsible for sawtooth oscillations. In TCV, sawteeth acquire a nonstandard character, as reported in Refs. [4]. When the ECRH power is deposited close to the q=1 surface, the line-integrated soft X-ray temporal traces exhibit non-standard shapes, which suggested the nickname *humpback* when they were first observed in T-10 experiments [5]. Our interpretation of this phenomenon is that specific features in the electron temperature profile are produced by localized ECRH. Then, the humpback behavior is consistent with the advection and the mixing of electron thermal energy in the plasma core associated with the excitation of resistive m=1 modes.

Figure 1 compares standard and humpback relaxation oscillations in TCV. Standard sawteeth, shown in Figs. 1a-b, are observed with auxiliary heating when the ECRH power is deposited on axis. Fig. 1a presents the line-integrated soft X-ray intensity, $I_X$, for the vertical chord through the plasma center as a function of time and Fig. 1b presents a tomographic reconstruction of the soft X-ray emissivity contours. With off-axis ECRH, different types of nonstandard oscillations (such as saturated sawteeth) are observed [4]. Humpback relaxations occur when the ECRH power is deposited close to the q=1 surface. The resulting humpback behavior for the line-integrated soft X-ray traces is shown in Fig. 1c. In Fig. 1d we show the corresponding emissivity isocontours. Humpback relaxation oscillations were also observed in T-10 with central electron cyclotron (counter)current drive [5]. However, current drive is not an essential ingredient for the appearance of humpbacks in TCV.

The distinctive feature of humback relaxations is the fast drop and rise of the central soft X-ray emissivity, on a time scale normally below 1 ms in TCV. We argue that the relaxation process, including the fast rise, is associated with the development of the m=1 instability. After the fast events, a diffusive and heating phase follows, during which the central emissivity is again observed to drop and rise, but on a slow time scale. The overall change in intensity is much smaller for a humpback than for a standard sawtooth for comparable ECRH power, safety factor and total plasma energy content, while the repetition time can be significantly longer.

One way to analyze soft X-ray data is the Singular Value Decomposition (SVD) method [6]. The inverted emissivity measurements form a signal matrix, $X$, which is decomposed into orthonormal spatial eigenvectors $u$ (*topos*) and temporal eigenvectors $v$ (*chronos*), resulting in a separation of variables $X(x,t) = \sum a_k u_k(x) v_k(t)$. The horizontal cuts of the three dominant pairs of eigenvectors characterizing a humpback oscillation are shown in Fig. 2. These can be interpreted as follows: $u_1$: average emission profile; $u_2$: profile peaking; $u_3$: m=1 structure. The $k = 1$ amplitude, $a_1$, is the largest by two orders of magnitude. The $k = 1$ chrono oscillates on the time scale of the humpback period. Between subsequent relaxations, the amplitude of the

$k = 2$ chrono is nearly constant as compared with its variation during the relaxations, which indicates that the X-ray emissivity does not show the typical peaking of standard sawteeth, but remains nearly flat within the q=1 region. The third pair of eigenvectors shows an m=1 oscillation which significantly exceeds the estimated noise level just before the relaxation phase. The different time behavior of the three eigenvectors suggests that the fast drop and rise of the relaxation phase is associated with MHD activity, while the slow oscillation phase is a global phenomenon of the emissivity profile, which can be ascribed to a transport process.

Our interpretation of the humpback phenomenon is based on the following heuristic picture. When the ECRH power is deposited near the q=1 radius, $r_1$, the temperature profile tends to become relatively flat, perhaps even hollow, in the central region up to the q=1 radius and relatively steep outside this radius, as the result of localized heating and diffusive transport during periods of relative MHD quiescence. These periods are terminated by the onset of m=1 magnetic islands. The formation of these features in the electron temperature profile requires relatively long quiescent periods, therefore improved stability against m=1 modes is an important factor. This improvement is possible because ECRH power deposited near the q=1 surface can lead to a reduction of the magnetic shear near that surface (via an increase of the local electrical conductivity), which is known from both experiments and theory [8] to produce a stabilizing influence.

Let us indicate with $T_0$, $T_1$ and $T_{mix}$ the values of the electron temperature before the onset of the m=1 magnetic island, on the magnetic axis, at the q=1 radius and at the sawtooth mixing radius [7] $r_{mix}$, respectively. For the case of a humpback, $T_0 \sim T_1 > T_{mix}$, while for a standard sawtooth $T_0 > T_1 > T_{mix}$. The m=1 magnetic island can grow on a time scale faster than the heating and diffusion time scales. Thus, during the island growth, the temperature on the displaced magnetic axis remains nearly constant, i.e. close to $T_0$. Similarly, the temperature at the island O-point remains close to $T_1$. The situation is illustrated in Figs. 3a,b. In Fig. 3a, the displacement, $\xi$, of the original magnetic axis is about $0.5 r_{mix}$. Since $T_0 \sim T_1$, both the plasma core and the island O-point region are relatively hot. Between these two peaks, a valley in the temperature profile is formed, with a minumum value, $T_{min}$, such that $T_1 > T_{min} \geq T_{mix}$. In fact, the inner and outer legs of the island separatrix are in thermal contact, as they are part of the same flux surface cross section, so that magnetic field lines on or near the separatrix connect central plasma regions with regions at a radial distance between $r_1$ and $r_{mix}$ from the center. This valley moves rapidly across the plasma center on the time scale of the island growth, as shown in Fig. 3b. Thus, the plasma temperature at a fixed central point drops and rises quickly during the passage of this valley, reproducing the fast drop-and-rise relaxation phase of a humpback. Note that, starting from a slightly hollow temperature profile peaked at $r_1$ (curve 1 of Fig. 3b), the relaxed profile is peaked on axis (curve 4), as the reconnection process in this case entails a net convection of thermal energy from the q=1 surface to the center. Then, a slow diffusive phase follows, during which the electron temperature on axis slightly drops and recovers as ECRH power is deposited off axis. The case of a standard sawtooth is contrasted in Figs. 3c,d.

Figure 3 is the result of a quantitative simulation model, first proposed in Ref. [3], which solves the thermal energy diffusion equation on flux tubes frozen to the plasma flow, taking into account a localized electron heat source, plasma rotation and a growing m=1 magnetic island. The magnetic topology is described by a helical flux function, $\psi_\star = \psi_\star(r, \alpha, \xi)$, where $\alpha = \theta - \phi$ and $\xi(t)$ is the radial displacement of the hot core magnetic axis. Figure 2 of Ref. [3] illustrates a poloidal cross-section of the $\psi_\star = const$ flux surfaces and the ECRH heating region. As a consequence of plasma rotation, the ECRH power is effectively deposited within an annular region comprised between the radii $r_{h1}$ and $r_{h2}$ on the poloidal midplane. At the particular instant in time when two surfaces with equal helical flux reconnect, a mixing rule for the thermal

energy is implemented [3]. In our model, the function $\xi(t)$ is a free parameter not determined theoretically. Reasonable trial functions for $\xi(t)$ are suggested by stability considerations and may be inferred from experimental data.

Typical simulation results for humpback oscillations are shown in Figs. 3a,b and 4. Input parameters are $r_{h1}/r_1 = 0.85$, $r_{h2}/r_1 = 1.15$, $\chi_\perp \tau_{saw}/r_1^2 = 0.2$ and $P_{EC}\tau_{saw}/(V_1 n) = 3 \times 10^{-16}$J, where $\chi_\perp$ is the cross-field thermal energy diffusion coefficient, assumed to be constant for $r \leq r_1$, $\tau_{saw}$ is the oscillation period, $P_{EC}$ is the ECRH coupled power and $V_1 = 2\pi^2 R {r_1}^2$. For instance, with $\tau_{saw} = 3ms$, $r_1 = 10cm$ and $n = 3 \times 10^{19} m^{-3}$, one obtains $\chi_\perp = 0.7 m^2/s$, a realistic value within the q=1 radius, and $P_{EC} = 500kW$. The function $\xi(t)$ used in this simulation is shown in Fig. 4a. Figure 4b shows the central electron temperature as a function of time. Humpbacks are obtained assuming heating near the q=1 radius and a relatively long period between successive relaxations with $\xi(t) \approx 0$, so that the electron temperature can build up in the region where the heating power is concentrated and $T_1$ can become comparable to or even larger than $T_0$. Figures 4c-d show simulated line integrated soft X-ray traces for two different vertical viewing chords: 4c is from a chord through the center and 4d is from a chord at a distance $0.4r_1$ from the center. The simulations in Figs. 3 and 4 give a fast drop and rise of the local electron temperature occurring on the same time scale. However, with a more structured functional form for $\xi(t)$, the fast rise can be made slower than the drop fase. This may be important for a more detailed comparison with the experimental traces, as will be shown in a forthcoming publication. Multi-peaked temperature profiles of the type observed in RTP [1] are obtained assuming narrower ECRH deposition widths and a magnetic island which grows slowly during a large fraction of the time between relaxations.

In conclusion, we propose an explanation of the humpback phenomenon based on specific features of the electron temperature profile produced by localized ECRH and on fairly standard model for m=1 magnetic islands. Indeed, in our model, the evolution of these islands obeys the topological constraints of the Kadomtsev model [7]. Yet, the humpback phenomenon was unforeseen and could be brought to light only with localized electron heating. The fast drop-and-rise of soft X-rays for a humpback is shown to occur during the growth of an m=1 magnetic island and the corresponding advection and mixing of thermal energy.

## References

[1] Lopes Cardozo, N. J., et al, *Phys. Rev. Lett.* **73** (1994) 256.
[2] Cima, G., et al, *Plasma Phys. Contr. Fusion* **40** (1998) 1149.
[3] Porcelli, F., et al, *Phys. Rev. Lett.* **82** (1999) 1458.
[4] Pietrzyk, Z. A., et al, *Nuclear Fusion* **39** (1999) 587.
[5] Razumova, K. A., et al, *Plasma Physics Reports* **23** (1997) 13.
[6] Dudok de Wit, T., et al, *Phys. Plasmas* **1**, (1994) 3288.
[7] Kadomtsev, B. B., *Fizika Plazmy* **1** (1975) 710.
[8] Porcelli, F., et al, *Plasma Phys. Contr. Fusion* **38** (1996) 2163.

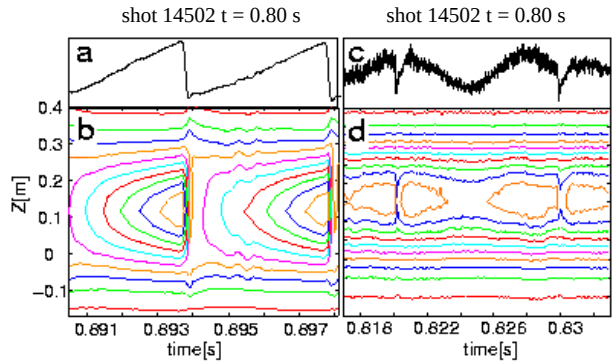


Figure 1: Standard (a,b) and nonstandard (c,d) central MHD activity in TCV. Frames (a) and (c): central soft X-ray line integrated intensity as a function of time; (b) and (d): soft X-ray emissivity isocontours.

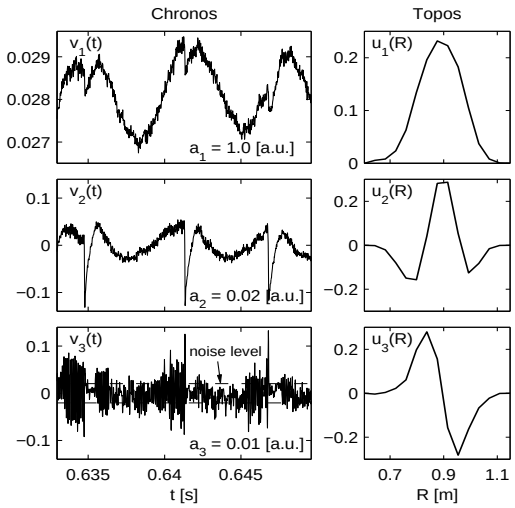


Figure 2: Singular value decomposition of soft X-ray emissivity for the case of a humpback oscillation.

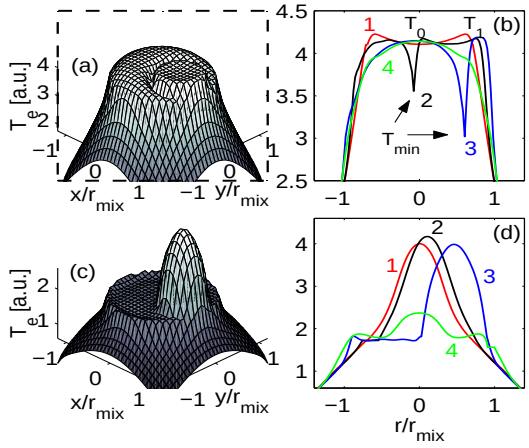


Figure 3: Simulation results. Humpback relaxation illustrated by (a): the temperature profile for a normalised displacement, $\xi = 0.53$, and (b): temperature profile sections through the island X and O points at $\xi = 0.14$ (curved marked 1), 0.53(2), 0.9(3) and 1.0(4). Standard sawtooth, illustrated by (c): the temperature profile at $\xi = 0.62$ and (d) sections at $\xi = 0.01(1)$, 0.15(2), 0.62(3) and 0.95(4).

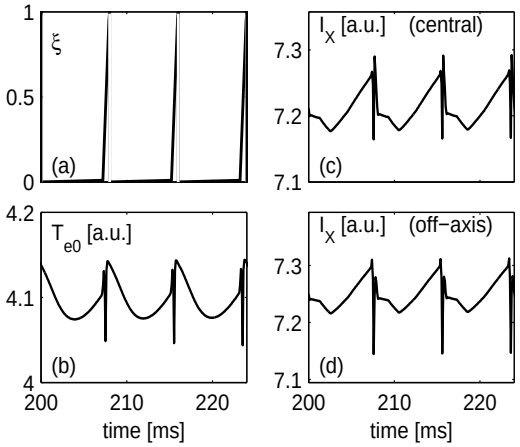


Figure 4: Simulation results, showing three periods of a humpback relaxation oscillation: (a) the assumed displacement function, $\xi(t)$; (b) central temperature evolution; (c) central and (d) off axis line integrated soft X-ray traces.